Convergence
A Journal for Young Researchers

ORIGINAL RESEARCH

Received: 7-28-25; Accepted: 11-27-25;
Managing Editor: Jonas Katona;
Action Editor: Steve Bullock

Remote Energy Monitoring via MQTT and SCT-013: A Single-Channel Prototype for IoT Systems

Pedro Henrique Dombi Xavier, Breno Gallego Martins, Murilo Campanharo Secco

Colégio Visconde de Porto Seguro, São Paulo, Brazil

Abstract

Growing pressure on Brazil's electrical systems—intensified by climate variability, rising demand, and limited access to affordable monitoring technologies—highlights the need for accessible tools that enable consumers to understand and manage their own energy use. This paper presents a low-cost, single-phase, non-invasive energy-monitoring prototype that leverages open-source hardware to provide real-time current and consumption data. The system employs the SCT-013 split-core current transformer to sense AC current via magnetic coupling, avoiding direct contact with mains wiring. An Arduino microcontroller (10-bit ADC, 0–5 V range) processes the conditioned analog signal produced across a 33 Ω burden resistor and midpoint-bias network, achieving a conservative measurement accuracy of ±5% across repeated trials (N = 5). An ESP32 module, synchronized to the Arduino over UART, handles wireless communication and publishes the processed data using the MQTT protocol, enabling multi-platform visualization through mobile applications, dashboards, and local LCD displays. The prototype's key contribution lies in combining non-invasive sensing, low-cost analog acquisition, and IoT-based data dissemination in a simple, reproducible architecture that can be assembled with widely available components. Results confirm stable measurement performance, reliable MQTT transmission, and a significantly lower cost compared to commercial smart meters. The system is applicable for residential, commercial, and educational environments, fostering awareness and reduction of unnecessary energy use. Limitations include dependence on network availability for remote access and support for single-phase monitoring only. Future work includes expanding to multi-phase systems, integrating cloud analytics, and applying machine learning for consumption prediction. By improving accessibility to real-time energy data, this project supports United Nations Sustainable Development Goal 7 (Affordable and Clean Energy) and demonstrates a practical pathway for promoting efficiency and technological inclusion.

Keywords: energy monitoring, Internet of things (IoT), MQTT protocol, SCT-013 current sensor, Arduino, ESP32

1. Introduction

Currently, from household lighting to the operation of large industries and infrastructure, energy serves as the driving force behind technological and social development. However, the increasing demand for electricity and the urgent need to reduce environmental impacts, combined with high production costs in Brazil, have made its availability an ever-growing challenge (Andrade, 2024; Pfeifer, 2018; Scianni et al., 2013).

In this context, climate change directly affects the efficiency of several renewable energy sources (Bento, 2024; Bitencourt, 2024; Scianni et al., 2013). On September 19, 2024, in Rio de Janeiro, the Electric Sector Monitoring Committee (CMSE) convened representatives from key agencies, including the Ministry of Mines and Energy, the National Electric Energy Agency (ANEEL), the National Agency of Petroleum (ANP), the Electric Energy Trading Chamber (CCEE), and the Energy Research Company (EPE), as well as technicians from the National Center for Monitoring and Alerts of Natural Disasters (CEMADEN) and the National System Operator (ONS). The meeting aimed to discuss, among other topics, the possible reintroduction of daylight-saving time in response to the country's ongoing energy generation crisis. The measure was proposed by ONS, which reported difficulties in meeting the growing demand for electricity (Andrade, 2024; Bitencourt, 2024; Rodrigues, 2024; Steil, 2024).

According to CEMADEN, rainfall measurements since 1950 indicate that Brazil is experiencing one of the driest periods in its recent history: the Northeast semi-arid zone has faced recurrent droughts, receiving 100-400 mm less rainfall per year than the historical average (Marengo et al., 2018), while model projections indicate that the Amazon basin could experience an increase in dry season length by up to 69% and a reduction in rainfall by 44% under combined deforestation and climate-change scenarios (Bottino et al., 2024). As a result, the generation capacity of hydroelectric plants has been reduced, forcing the country to turn to alternative sources (Steil, 2024). Additionally, due to the unpredictability of wind patterns, ONS states that it is not feasible to fully rely on wind energy to meet demand (Bitencourt, 2024). Consequently, Brazil has increased its reliance on thermoelectric plants, raising emissions by ~9% and increasing energy costs for consumers (Andrade, 2024; Bitencourt, 2024; Rodrigues, 2024).

The proposed return of daylight-saving time aims to mitigate the effects of the so-called "ramp effect," a period of peak energy demand between 6 p.m. and 7 p.m. (Andrade, 2024). During this window, almost the entire thermoelectric system is activated, which, according to the Minister of Mines and Energy, Alexandre Silveira, directly influences final costs for consumers. The reinstatement of daylight-saving time could relieve pressure on the National Interconnected System (SIN) by extending solar energy production and reducing reliance on thermoelectric plants, while also encouraging the use of natural light, decreasing the need for electric appliances (Bitencourt, 2024).

According to ONS, adopting daylight-saving time could reduce peak electricity demand in Brazil by up to 2.9% (Andrade, 2024). Moreover, thermoelectric plants not only pollute the environment but also raise the marginal cost of operation (CMO) to R$1,248/MWh (US$224.14/MWh), whereas the cost before their activation was below R$500/MWh (US$89.80/MWh) (Bitencourt, 2024). ONS estimates that reinstating daylight-saving time could generate savings of up to R$400 million (approximately US$71.8 million) between October 2024 and February 2025, benefiting both the government and the population by lessening the impact of electricity cost increases (Andrade, 2024).

These challenges are directly related to our project and to the United Nations' 2030 Agenda, particularly Sustainable Development Goal (SDG) 7, which aims to ensure universal access to reliable and modern energy services, increase the share of renewable energy in the global energy matrix, and promote international cooperation in clean technologies (United Nations Brazil, 2024).

Given the increasing pressure on Brazil's energy system and the rising cost of consumption during peak hours, demand-side monitoring has become an essential tool for identifying waste, improving efficiency, and reducing unnecessary stress on the grid.

In this scenario, real-time consumption monitoring becomes a practical mechanism for managing demand and promoting consumer awareness. Although advanced monitoring systems—such as Sense Energy Monitor, Emporia Vue, or LoRaWAN-based meters used in Europe—are well established internationally, these solutions remain costly, depend on proprietary infrastructure, or require professional installation. Most Brazilian households lack access to similarly affordable, transparent, and easily deployable technologies. This creates a clear technological and socioeconomic gap: low-cost, clamp-on, open-source monitoring solutions adapted to Brazil's grid and climatic conditions are scarce. The present prototype—by enabling industries, businesses, and households to monitor their energy consumption—is designed to address precisely this gap, offering an accessible and reproducible tool that promotes financial savings while helping to mitigate the "ramp effect." Together, these components form a technically efficient and economically viable architecture aligned with Brazil's energy monitoring challenges.

Unlike invasive measurement approaches, the system utilizes the clamp-on current sensor SCT-013 that measures the magnetic field variation around a conductive wire and converts this data into a current proportional to the original. This current is then transformed into signals that can be processed by an Arduino microcontroller, which interprets the readings. The data is subsequently transmitted over a network, where the Arduino communicates with an ESP32—a more advanced microcontroller with higher processing capacity. The data can be accessed via a real-time application from anywhere in the world, enabled by the MQTT (Message Queuing Telemetry Transport) protocol, which ensures efficient data transmission to an external server (Sasaki & Yokotani, 2019; Silva et al., 2021). MQTT enables fast and reliable communication between devices: the ESP32 publishes the collected data to the server, and connected devices can subscribe to topics to receive this information in real time (Sasaki & Yokotani, 2019; Silva et al., 2021). Designed to optimize bandwidth use and reduce power consumption, MQTT is ideal for Internet of Things (IoT) applications, where efficiency and reliability are essential (Sasaki & Yokotani, 2019; Silva et al., 2021). By focusing on real-time waste identification, the system empowers users to make immediate and informed decisions, optimizing energy use in a practical and accessible manner, essential in Brazil's context (Pfeifer, 2018; Rovere, 2016; Tamkittikhum et al., 2015; Thakare et al., 2016).

Contrary to these commercial or proprietary systems, the proposed prototype emphasizes accessibility and transparency while maintaining technical rigor. It employs open-source hardware and software, enabling full replication and modification by students, technicians, and researchers, thereby bridging the gap between academic learning and practical energy management. Furthermore, built with low-cost and widely available components—such as the SCT-013 split-core current transformer, Arduino, and ESP32—the system can be installed without electrical intervention or specialized labor, ensuring safety and ease of use. The data visualization through the MQTT protocol and multiple display formats, such as LCD panels and web-based interfaces, evince the accessibility of the project. Designed with the Brazilian energy context in

mind—particularly the "ramp effect" and reliance on hydropower—the project promotes awareness and control over electricity consumption. By adopting a very easy and safe installation approach, it achieves measurement reliability comparable to commercial systems at a fraction of the cost, offering a socially inclusive solution aligned with the United Nations' 2030 Agenda for Sustainable Development.

2. Literature Review

2.1. Theoretical Foundation

The prototype relies on fundamental principles of electricity and magnetism, particularly Ohm's Law and Faraday's Law of electromagnetic induction. According to Ohm's Law, the relation between voltage V, current i, and resistance R is $V = iR$, forming the basis for quantifying current flow in a resistive circuit. Likewise, Ampère's Law states that an electric current produces a magnetic field B around the conductor, which decreases with distance r as $B = \mu_0 I/2\pi r$.

When this magnetic field varies over time, Faraday's Law predicts an induced electromotive force (EMF):

$$EMF = -\frac{d\Phi_B}{dt},$$

$$\Phi_B = \int \vec{B} \cdot d\vec{A},$$

where Φ_B is the magnetic flux. In practice, this means that a conductor carrying AC current generates a time-varying magnetic field that can be detected without direct electrical contact.

Magnetically coupled current sensors, such as the SCT-013 transformer used in this work, exploit this principle: the alternating magnetic field around a single-phase conductor induces a proportional voltage in the sensor's coil (Miron-Alexe, 2016; Sanket et al., 2016). This voltage, after conditioning through a burden resistor and analog-to-digital conversion, allows real-time current estimation while maintaining electrical isolation and safety.

SCT-013 Current Sensor

Current transformers such as the SCT-013 have become standard in low-cost monitoring systems because they combine galvanic isolation, adequate linearity for residential load ranges, and magnetic clamp-on measurement (Miron-Alexe, 2016; Sanket et al., 2016). These characteristics are particularly relevant in contexts like the Brazilian residential sector, where access to professional installation is limited and safety concerns discourage intrusive sensing methods. The literature consistently highlights that the sensor reduces installation risk, improves user adoption, and maintains compatibility with low-power microcontrollers—all priorities that directly shaped the architecture of the present project. The SCT-013 operating principle relies on detecting variations in the magnetic field generated by alternating current in the conductor and inducing a proportional secondary current in the coil, as illustrated in Figure 1. This sensing model enables accurate current estimation, a key requirement for scalable and user-friendly energy monitoring solutions (Miron-Alexe, 2016; Sanket et al.,

2016).

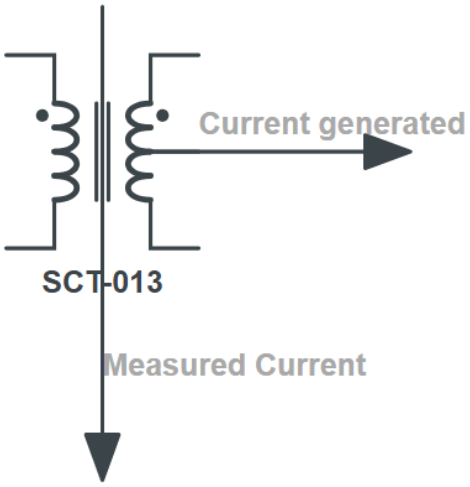

Figure 1: Diagram illustrating the measured current and the generated current. Source: Authors

Reading the data collected from the sensor is possible by the integration of an Arduino, a microcontroller that converts this data. The SCT-013 sensor outputs an AC current signal that oscillates around zero, including negative voltages, which can be shown in Figure 2 (Miron-Alexe, 2016; Sanket et al., 2016). However, since the Arduino is limited to reading only positive voltages (0-5V) on its analog input, the signal is necessarily shifted upward (Miron-Alexe, 2016; Sanket et al., 2016).

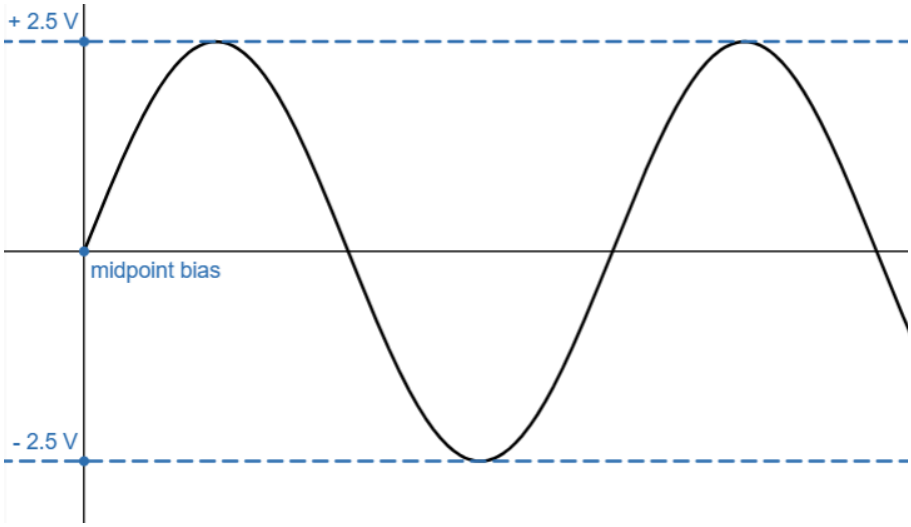

Figure 2: Alternating current graph (-2.5V to +2.5V). Source: Authors

Following these established conditioning principles (Miron-Alexe, 2016; Thakare et al., 2016), the prototype applies a voltage-biasing network (Figure 4) that shifts the sensor output to a 2.5 V midpoint, generating a waveform centered within the 0-5 V range of the Arduino's ADC (Figure 3).

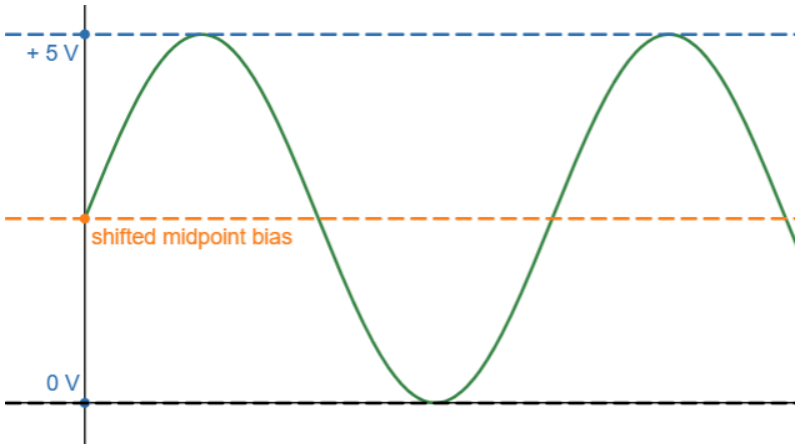

Figure 3: Alternating current graph (0V to +5V). Source: Authors

The signal conditioning circuit consists of:

- A 100µF electrolytic capacitor, which filters and stabilizes the bias voltage.
- Two 10kΩ resistors forming the voltage divider.
- A 33Ω burden resistor, which converts the current output from the SCT-013 into a proportional voltage.

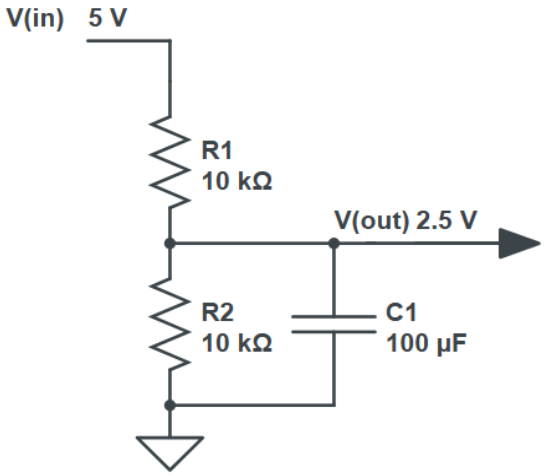

Figure 4: Voltage divider scheme. Source: Authors

Convergence
A Journal for Young Researchers

Proper signal conditioning is essential for ensuring both measurement fidelity and compatibility between the SCT-013 output (current) and the Arduino's analog-to-digital converter. Because the sensor operates as a current transformer, its output must first be converted into a voltage before connecting the signal to the voltage divider. This requirement is emphasized throughout the literature, which consistently notes that burden resistor selection plays a central role in determining linearity, noise performance, and ADC safety margins in current-sensing systems (Sanket et al., 2016; Thakare et al., 2016).

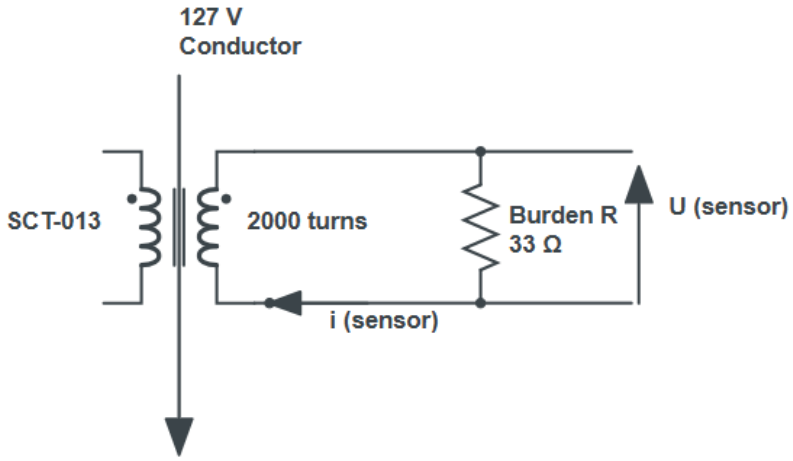

Figure 5: Electrical diagram of the SCT-013 sensor in parallel with the calibration resistor. Source: Authors

The burden resistor is placed directly across the SCT-013 terminals (Figure 5), ensuring that the induced current is translated into a proportional voltage prior to biasing. To avoid clipping after midpoint shifting, the peak sensor output must remain within the ADC's readable range (0-5 V). The burden value was therefore derived using Ohm's Law to constrain the maximum expected voltage to approximately ±2.5 V, yielding a theoretical resistance of 35.4 Ω.

$$R = V\,(\text{analog input}/2)/I\,(\text{sensor}) = 2.5\ \text{V}/0.0707\ \text{A} = 35.4\ \Omega$$

Since this value is not commercially standard, a 33 Ω resistor was adopted.

After conversion by the burden resistor, the signal is integrated into the biasing network composed of two 10 kΩ resistors and a 100 µF capacitor (Figure 4), which establishes a stable 2.5 V midpoint and filters low-frequency noise. This configuration produces a conditioned waveform fully contained within the 0-5 V input range while preserving proportionality between the measured current and the sensed magnetic field.

The complete electric circuit is configured as illustrated in Figure 6.

For the measurements to be reliable, the Arduino must convert the voltage generated across the burden resistor into an estimate of the primary current through the EmonLib library. This requires a calibration constant that reflects the physical

characteristics of the SCT-013. Since the sensor outputs current, the burden resistor (33 Ω, chosen as the closest value to the theoretical 35.4 Ω) defines the proportional voltage read by the ADC.

CalibrationValue = number of turns of the sensor/value of load resistor
CalibrationValue = 2000/33
CalibrationValue = 60.606

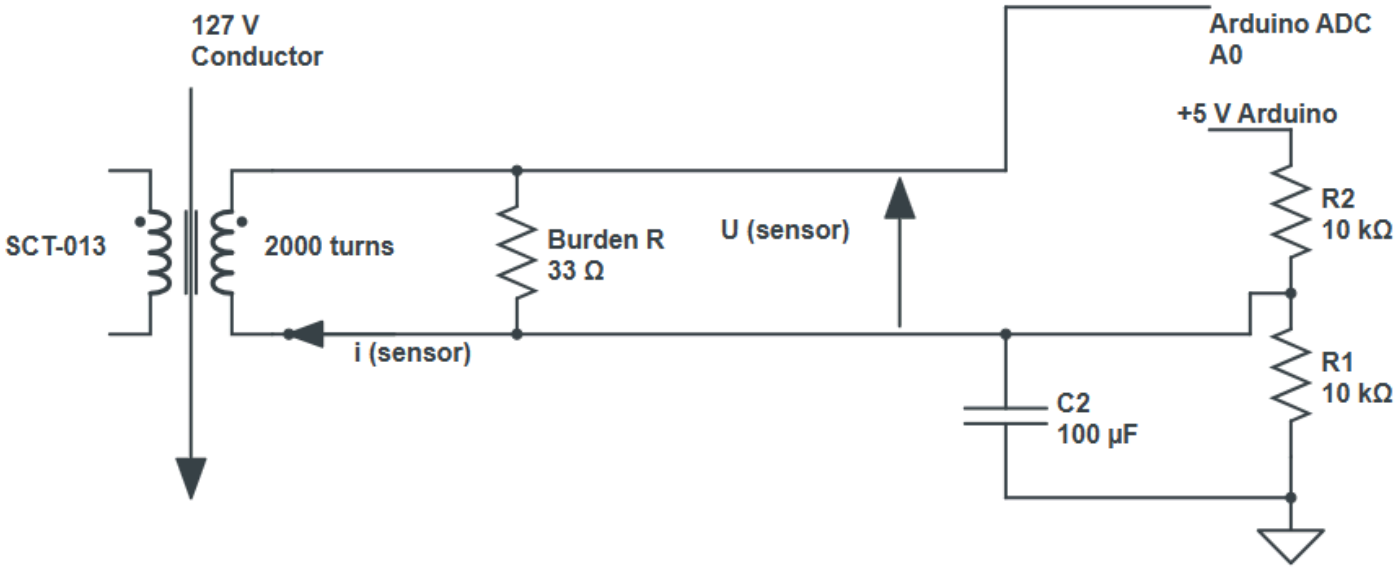

Figure 6: Final electric circuit Source: Authors

The Arduino's serial communication is initialized with 9600 (baud rate), which refers to the number of bits transmitted or received per second.

SCT013.current(pinSCT, 60.606);

It is important to note that this calibration value is used with Arduino, which has a 5V analog input.

The entire code to print data at Serial Monitor is available in the GitHub repository: https://github.com/Peagudoo/Monitoring-Project-Code/blob/main/Arduino_test_Serial_print_example

Accurate sensing also requires placing the SCT-013 around only one conductor. If both phase and neutral pass through the core, their magnetic fields cancel, producing zero net flux and preventing measurement. This condition is fundamental to all split-core current transformers.

Arduino and ESP32 Synchronization

The initial objective of the project was to avoid using Arduino and instead rely solely on the ESP32, a microcontroller with greater processing power and a wider range of features. This choice was made to enable the integration of IoT into the system with a data analysis interface, allowing users to monitor their electricity consumption at any time and from anywhere in the world.

Advantages of integrating the ESP32 into the project (Maier et al., 2017):

- **High Processing Capacity:** The ESP32 features a dual-core processor with speeds up to 240 MHz, enabling rapid processing of large volumes of data collected by the current sensor.
- **Built-in Wi-Fi and Bluetooth Connectivity:** Integrated Wi-Fi allows the ESP32 to connect to local networks or the internet, facilitating data transmission to external servers and applications. Bluetooth functionality enables communication with nearby mobile devices, allowing quick configuration and local data transfer when necessary.
- **Compatibility with the MQTT Protocol:** The ESP32 supports the MQTT protocol, which is highly efficient for data transmission in IoT applications. MQTT allows lightweight and fast communication, essential for real-time energy consumption data transmission. This compatibility ensures the system can continuously and reliably send and receive data, minimizing delays and maximizing communication efficiency.
- **Expandable Storage and Memory Capacity:** With internal flash memory and support for expansion, the ESP32 can temporarily store large amounts of data in case of connection interruptions with the server, preventing the loss of important information.

The storage capacity allows the implementation of local algorithms for data pre-processing, reducing the amount of information sent to the cloud and saving bandwidth (Maier et al., 2017). When evaluating the feasibility of using the ESP32 as the sole acquisition device, the burden resistor is recalculated to match its 3.3 V ADC reference. The lower ADC range requires a burden sized for a ±1.65 V swing, which corresponds to approximately 23.3 Ω for the expected 70.7 mA secondary peak. In practice, the closest standard value (22 Ω) was used, and the calibration constant was adjusted accordingly to preserve proportionality.

$$R = V_{(analog\ input/2)}/I_{(sensor)} = 1.65\ V/0.0707\ A = 23.33\ \Omega\ (closest\ resistor\ value\ in\ the\ market:\ 22\ \Omega)$$

CalibrationValue = number of turns of the sensor/value of load resistor
CalibrationValue = 2000/22
CalibrationValue = 90.909

```
SCT013.current(pinSCT, 90.909);
```

To verify the accuracy of measurements using the ESP32, the collected data were compared to those obtained with a professional clamp ammeter. However, the results were unsatisfactory, as the ESP32 readings varied substantially compared to the reference values. The reason for such discrepancy is discussed in the Limitations section. Hence, the final measurement chain employs the Arduino for analog sampling and conversion, with the ESP32 dedicated exclusively to wireless serial communication via UART. This approach allows the ESP32 to manage the network and, consequently, provide

remote access for users to view the measured data.

Serial Communication

The UART (Universal Asynchronous Receiver/Transmitter) digital communication method is employed, which allows data exchange between two devices—Arduino and ESP32 (Gupta et al., 2020).

Main Characteristics (Gupta et al., 2020):

1. **Asynchronous:** It does not require a shared synchronization clock between devices. Instead, data is transmitted with a fixed format and baud rate, and the receiver must recognize and interpret the timing based on these parameters.
2. **Data Transmission:** Data is transmitted bit by bit in sequence. This can be done in two ways:
    - TX (Transmission): The device sends data.
    - RX (Reception): The device receives data.

Operation (Gupta et al., 2020):

1. **Data Transmission:** The transmitter sends a data byte preceded by a start bit and followed by stop bits. The data byte is sent bit by bit, starting with the least significant bit.
2. **Data Reception:** The receiver waits for the start bit, then collects the data bits and stop bits to reconstruct the original byte.

UART establishment is based on the SoftwareSerial library, which is responsible for defining RX (Receiver) and TX (Transmitter) pins.

```
SoftwareSerial serialBT(2,3); // RX(Arduino)-3 and TX(Arduino)-2
```

Arduino's serial initialization of data transmission is performed at a speed of 9600 bits per second.

```
serialBT.begin(9600);
```

Transmission of collected data to the ESP32 via UART occurs using print commands.

```
serialBT.print(current);
```

ESP32 receives data after two separate serial communications are initiated: one to receive data from the Arduino (Serial2.begin), and another to send data to the computer (Serial.begin) for viewing via the Arduino IDE's serial monitor.

```
Serial.begin(9600); // Initializes serial communication with the computer's serial monitor at a baud rate of 9600.
Serial2.begin(9600, SERIAL_8N1, 18, 5); // RX(ESP32)-D18 and TX(ESP32)-D5
```

Adjustments with desired variables in the standard program enable the correct interpretation of data sent by the Arduino and

received by the ESP32.

The code is detailed in the GitHub repository: https://github.com/Peagudoo/Monitoring-Project-Code/blob/b978bf0b2189e62114fa00f6bf7182c91115bbd6/ESP32_RecieveData-FromArduino_example

To make the data stored in the memory of both microcontrollers available in a user-friendly interface, the MQTT protocol is implemented, which is responsible for storing data on an external server connected to the network. Accordingly, the ESP32 transmits the data to the network, and an application collects this data on its interface, allowing the user to access information about their electricity consumption.

MQTT Protocol

The MQTT protocol establishes communication between client and server, where the client can both store and receive data (Sasaki & Yokotani, 2019; Silva et al., 2021). This is achieved through a Publish-Subscribe method, which involves a Broker—an intermediary information server that receives data sent from sensors, manages it, and shares it according to the client's needs, as can be seen in Figure 7.

The client acts in two distinct roles: as a Publisher (posting data) and as a Subscriber (receiving data). The relationship between the client and the Broker functions such that the Broker organizes received information in a hierarchical system according to topics. Clients can subscribe to the topics they wish to receive; however, the Broker manages the requests, so the Client and Publisher do not communicate directly, thereby maintaining anonymity for both parties (Sasaki & Yokotani, 2019; Silva et al., 2021).

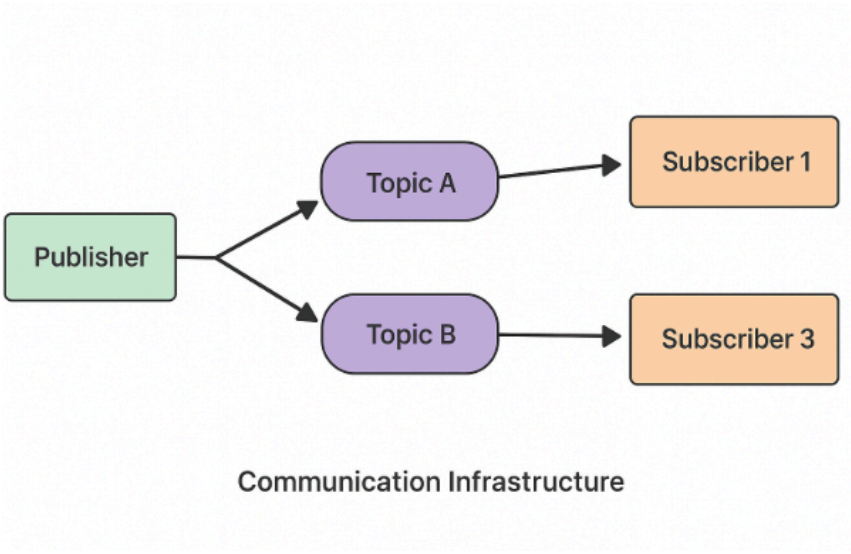

Figure 7: Communication diagram using the MQTT protocol. Source: Authors

In the project, the following topics are used: electric current, energy, cost, and power, with each item representing a specific topic. The Publisher is the ESP32, which, upon receiving data collected from the Arduino, sends it to the Broker. The client is the application, which requests data from the Broker, and the Broker, in turn, delivers the data.

Advantages of the MQTT Protocol:

- Low memory consumption
- Low processing requirements
- Low bandwidth usage
- Low latency
- High reliability (Sasaki & Yokotani, 2019; Silva et al., 2021)

Since the Publisher does not send information directly to clients, it does not need to store client information or send multiple copies of data—only the specific data requested. Additionally, only information related to the Broker, its topics, and packet transmissions is stored. For these reasons, MQTT is excellent for IoT applications, providing a low-cost and accessible solution for projects handling moderate amounts of data (Sasaki & Yokotani, 2019; Silva et al., 2021).

Beyond these well-known benefits, recent evaluations confirm MQTT's scalability in large deployments. For example, Silva et al. (2021) demonstrated that MQTT brokers can handle up to 500 simultaneous clients publishing in parallel while maintaining latency below 200 ms per message, with stable throughput of several thousand messages per second. Under broker load tests with Mosquitto (a lightweight, open-source MQTT broker widely used for IoT applications) and EMQX (a high-performance, enterprise-grade MQTT broker), the system sustained low packet loss and CPU usage below 70%, even during peak conditions. Furthermore, MQTT supports reliable Over-the-Air (OTA) firmware updates—that is, the remote distribution and installation of new firmware onto devices without physical access—exceeding 100 KB with more than 99% success rate when QoS (Quality of Service) levels 1 or 2 were enabled (Silva et al., 2021). QoS 1 guarantees that a message is delivered at least once, while QoS 2 ensures it is delivered exactly once, providing stronger reliability in critical applications (Silva et al., 2021). These results reinforce that MQTT is not only suitable for small-scale prototypes such as ours but also inherently capable of scaling to multi-device and multi-channel energy monitoring systems, maintaining efficiency, low latency, and reliability in scenarios ranging from household deployments to large smart grid infrastructures (Silva et al., 2021).

3. Methodology

3.1. Prototype Development

The prototype was developed to emulate a typical single-phase electrical installation, enabling the monitoring of both total and individual circuit consumption, not merely as a physical layout but as a methodological framework for validating multi-point energy monitoring. The experimental setup consists of four circuit breakers: one main breaker that supplies the entire system—allowing total energy measurement through a single SCT-013 sensor—and three auxiliary breakers dedicated to specific electric devices, as seen in Figure 8. This arrangement provides controlled segmentation of the electrical network, enabling simultaneous evaluation of whole-circuit measurements and per-device monitoring. By emulating common residential or small commercial configurations, the prototype allows the system to be tested across diverse load scenarios,

supporting verification of measurement consistency and sensor responsiveness.

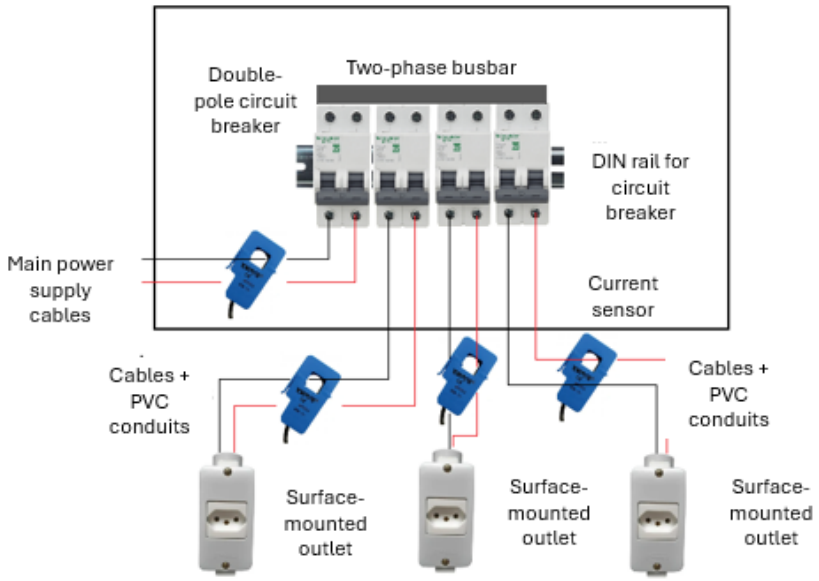

Figure 8: Initial sketch of the project. Source: Authors

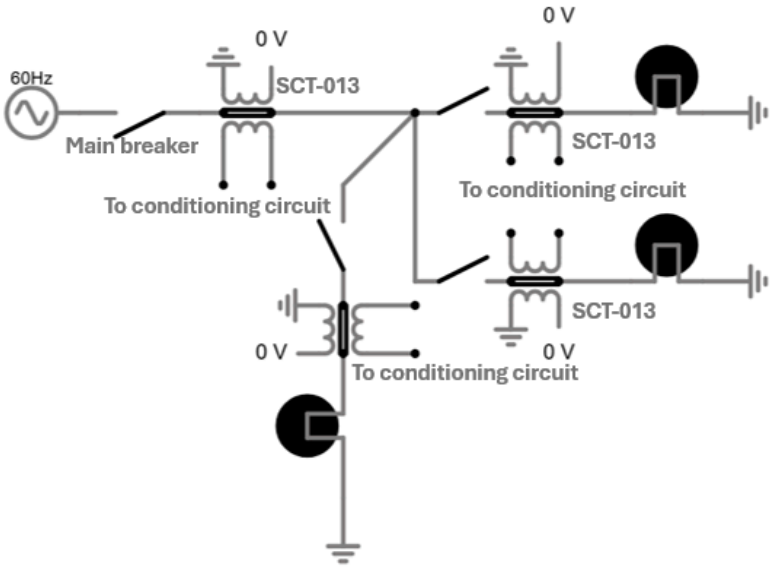

Figure 9: System overview circuit diagram. Source: Authors

The components were arranged on a wooden panel designed to replicate the spatial organization of a real electrical distribution board, allowing controlled and safe validation of the monitoring architecture. The power box housed the sensing and processing units—including the SCT-013 sensors, the Arduino microcontroller, and the ESP32 module—while maintaining physical separation from the energized conductors to ensure electrical isolation.

Each current sensor was clamped around the selected conductor. To support offline usability and provide immediate feedback to users, four LCD modules were installed to display real-time current values for each monitored branch, as illustrated in Figure 10. Their placement beside the corresponding outlets was intentional, facilitating intuitive association between visualized consumption and the physical circuit being measured.

Figure 10: Image of the wooden panel and the power box (left), as well as the LCD display to display real-time readings (right). Source: Authora

The circuit is powered by a switched-mode power supply that converts 127 V AC mains input into a stable 12 V DC output. A voltage regulator limits this to approximately 6.5 V to protect the microcontrollers.

The passive components—resistors, capacitors, and connectors—were assembled on a prototyping board, and together with the Arduino and ESP32 were enclosed within the power box for safety and organization, as seen in Figure 12. The circuit connections to the four current sensors extend outside the power box, allowing for measurement of the electrical conductor wires.

It is important to note that, in this laboratory setup for panel creation, the microcontrollers were powered directly from the main supply solely to ensure stability during extended testing. In practical deployments, however, no electrical intervention in the building's wiring is required. The system can operate using external DC adapters or portable battery packs, both of which provide sufficient energy only for short-term use. However, because microcontrollers such as the Arduino and ESP32 support deep-sleep and interrupt-based operation, the system can be programmed to sample current periodically rather than continuously. By remaining active only for brief measurement and transmission intervals—on the order of

Convergence
A Journal for Young Researchers

microseconds—these devices can reduce average consumption from tens of milliamperes to the range of microamperes between cycles. Therefore, fully non-intrusive powering strategies may be adopted to eliminate reliance on external power outlets. One promising approach involves the use of dedicated inductive or magnetically coupled energy-harvesting modules—independent of the SCT-013—that capture a small fraction of the electromagnetic field around the mains conductor. After rectification and storage, this harvested energy can sustain low-power embedded systems while maintaining complete isolation from the electrical circuit. Although not implemented in this prototype, such methods are fully compatible with the system architecture and represent a logical direction for future iterations.

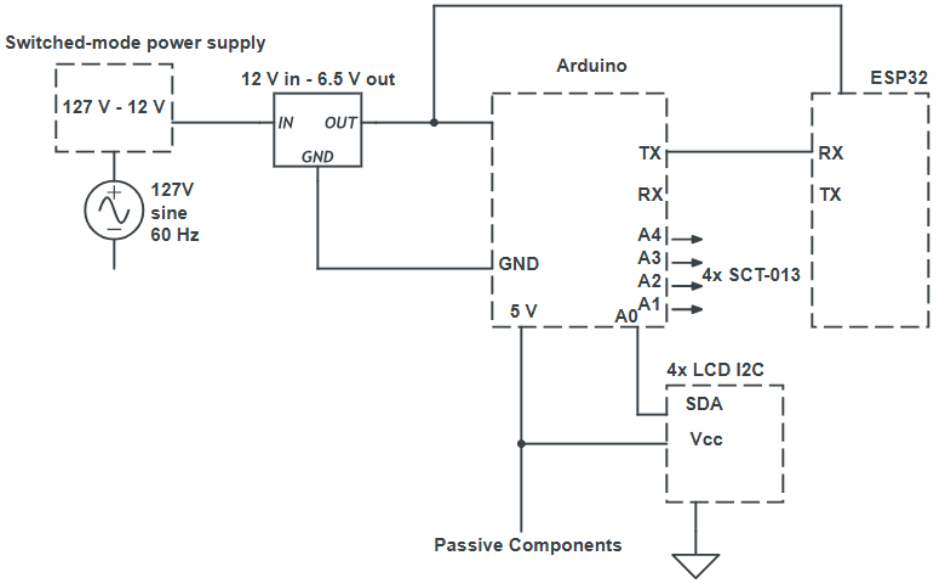

Figure 11: Power and communications circuit. Source: Authors

The final circuit configuration connects the main power line to the primary circuit breaker, which distributes the 127 V AC supply to three independent outlets corresponding to the monitored loads, as seen in Figures 8 and 9. In parallel, the mains voltage feeds a switched-mode power supply that converts 127 V AC to 12 V DC. A subsequent voltage regulator limits the output to 6.5 V to ensure safe operation of the Arduino, ESP32, LCD displays (Figure 11), and signal-conditioning board (Figure 6).

System control is achieved through firmware developed for both microcontrollers. The Arduino handles analog signal acquisition from the SCT-013 current sensors, while the ESP32 manages data transmission and communication via the MQTT protocol. This configuration allowed the system to be tested under realistic and traceable consumption patterns, enabling validation of sensor behavior across separate branches of the installation.

The definitive source codes are available in the project's public repository.

Arduino: https://github.com/Peagudoo/Monitoring-Project-Code/blob/main/Final_Arduino_code

ESP32: https://github.com/Peagudoo/Monitoring-Project-Code/blob/main/Final_ESP32_code

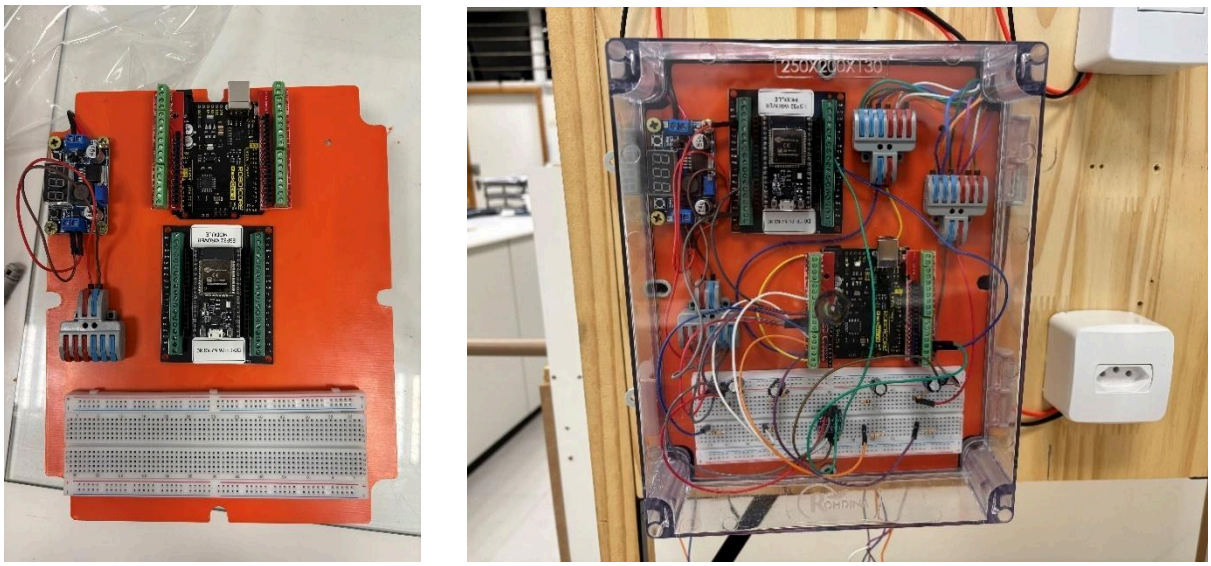

Figure 12: Image of the electrical box, with its respective connections. It is not possible to observe the current sensors and their connections in this image. Source: Authors

3.2. Testing

The prototype performance was validated using three complementary visualization modes: (1) local LCD displays, (2) an MQTT-based mobile application, and (3) a web interface hosted on the ESP32. These approaches ensured both on-site and remote data verification.

LCD Display Testing

To verify measurement accuracy, sensor readings were compared against a calibrated clamp ammeter. Tests were performed under controlled load conditions including resistive devices such as lamps and soldering irons. The LCD interface, implemented via the LiquidCrystal_I2C library, displayed real-time data from the SCT-013 sensors, as seen in Figure 13.

Four 20×4 LCD modules were individually addressed to represent the four monitored circuits. Object declaration follows the standard format of the library.

```
LiquidCrystal_I2C lcd1(address, n_columns, n_rows); // object that controls the LCD display
LiquidCrystal_I2C lcd1(0x24, 20, 4); // example
```

The parameters correspond respectively to the device address, number of columns, and number of rows. Display initialization and backlight activation are required.

```
lcd1.init();
lcd1.backlight();
```

Each LCD presented one variable per line, enabling direct observation of instantaneous current values. The complete code routine is available in the public repository: https://github.com/Peagudoo/Monitoring-Project-Code/blob/main/LCD_Display_Printing_Example

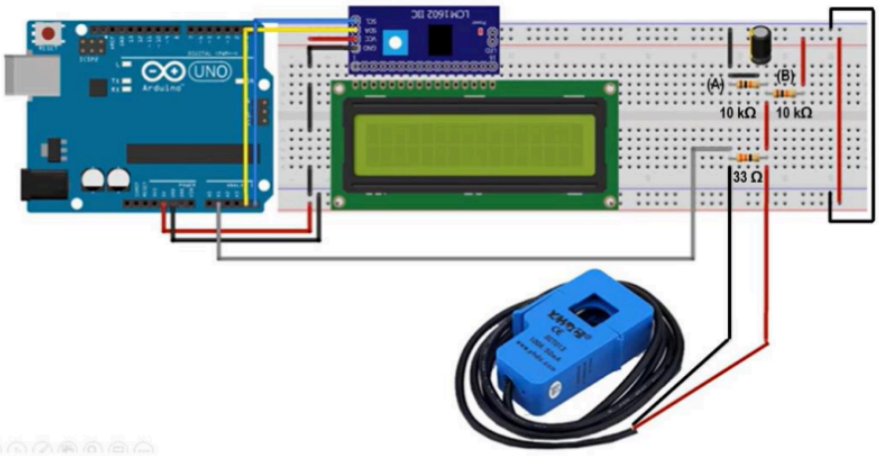

Figure 13: Use of the LCD display to visualize data from the SCT-013. Source: Authors

Preliminary tests focused on quantifying the deviation between the SCT-013 measurements and a professional clamp ammeter, establishing the baseline accuracy of the signal-conditioning chain. At this stage, only one sensor-LCD pair was used, isolating the current-measurement subsystem from other elements such as serial communication or MQTT transmission. This isolation allowed us to verify whether observed deviations originated from the sensor, the conditioning circuit, or external environmental factors.

Test performed with a lamp:

- Value measured by the SCT-013 sensor: 160 mA
- Value measured by the clamp ammeter: 120 mA
- Margin of error: 33%

Test performed with a soldering iron:

- Value measured by the SCT-013 sensor: 160 mA

- Value measured by the clamp ammeter: 120 mA
- Margin of error: 33%

Two controlled load tests were conducted (lamp and soldering iron), which produced comparable deviations (33%). The consistency of this deviation suggested a systematic rather than random source. Notably, the sensor exhibited non-zero readings even in the absence of a load when tested in the laboratory environment.

When the same setup was tested outside the laboratory—an environment with lower electromagnetic congestion—the sensor correctly returned zero current in no-load conditions and accuracy improved substantially. This contrast reinforced the conclusion that external electromagnetic interference was influencing the sensor output. The SCT-013, being a magnetically coupled device, is sensitive to ambient fields generated by nearby electronic equipment. Identifying this effect was essential for validating the need for shielding and for interpreting measurement uncertainties in controlled experiments.

Application Testing using the MQTT Protocol

With the Arduino-ESP32 synchronization validated and the ESP32 fully integrated with the MQTT protocol, we were able to assess the system's remote-monitoring performance. MQTT was selected because its lightweight publish-subscribe architecture minimizes bandwidth usage and ensures reliable transmission even under unstable network conditions—an essential requirement for real-time energy monitoring from anywhere in the world (Sasaki & Yokotani, 2019; Silva et al., 2021).

To evaluate data delivery—from sensor acquisition to user-level visualization—the developed system used the ON OFF iOS application as the MQTT client. This platform allowed us to verify whether the ESP32, acting as the publisher, could consistently deliver data to an external broker and whether the client could retrieve and display measurements without loss, delay, or formatting inconsistencies.

For testing purposes, only the measurement from the main circuit breaker (total current of the installation) was published during testing. Focusing on a single channel simplified the validation of communication robustness, eliminating internal confounding factors. This ensured that any observed latency or discrepancy originated from the network path—not from the sensing chain.

This link contains an MQTT video test: https://docs.google.com/presentation/d/1d3qZIVl55eJ1PHWbBPnyKwMF6CbK8FIfDjc_fjMUi6Q/edit?usp=sharing

Web Interface Testing

A web server was implemented on the ESP32 so that consumption data can be accessed remotely via a standard HTTP interface. This allows users to monitor energy usage in real time from any browser on the network. This dual-interface strategy—MQTT and HTTP—was implemented not as an additional feature but as a test of system robustness and flexibility. By verifying that the ESP32 could simultaneously handle data reception from the Arduino, local processing, and HTTP-based data delivery, we assessed whether the overall architecture could support heterogeneous user environments—ranging from lightweight IoT dashboards to conventional browser-based access.

The code is available at the following GitHub repository: https://github.com/Peagudoo/Monitoring-Project-Code/blob/main/WebServer_test_code

Test video with the web server: https://docs.google.com/presentation/d/1n3twGLn_ofM23tX9RS8k1i5nGzYXelZxA8VGZgHaPw0/edit?usp=sharing

4. Results

An analysis of the margin of error for various electrical appliances was conducted and then compiled into Table 1. Additionally, a comparative graph between the clamp-on current sensor and the clamp ammeter was created, as shown in Figure 14, and a correlation plot in Figure 15, illustrating how the measurement error varies with the current measured by the SCT-013.

Table 1: Comparative table with data collected from SCT-013 and professional clamp ammeter. Source: Authors

No.	Devices	SCT-013 (A)	Professional clamp ammeter (A)	Deviation	Margin of Error	N (measurements taken)	SD (A)
1	Sterilair Air Purifier	0.26	0.25	0.01	4%	5	0.009
2	LG SmartTV	0.62	0.65	-0.02	-5%	5	0.012
3	Arno Fan (low power)	0.64	0.65	-0.01	-2%	5	0.011
4	Arno Fan (medium power)	0.82	0.82	0.00	0%	5	0.012
5	Arno Fan (high power)	1.07	1.08	-0.01	-1%	5	0.013
6	Blender (low power)	1.44	1.46	-0.02	-1%	5	0.015
7	Consul Refrigerator	1.60	1.63	-0.03	-2%	5	0.016

8	Blender (high power)	1.74	1.75	-0.01	-1%	5	0.016
9	Philco Vacuum cleaner	3.32	3.33	-0.01	0%	5	0.021
10	Conair Hair Dryer (low power)	3.45	3.50	-0.05	-1%	5	0.020
11	Philco Hair Dryer (high power)	4.35	4.38	-0.03	-1%	5	0.020
12	Conair Hair Dryer (high power)	6.22	6.30	-0.08	-1%	5	0.021
13	Philco Hair Dryer (high power)	8.20	8.40	-0.20	-2%	5	0.022
14	Cadence Electric Kettle	8.31	8.46	-0.15	-2%	5	0.022
15	Microwave Oven	12.14	12.70	-0.56	-4%	5	0.025

The average margin of error is at most ±5%.

As summarized in Table 1 and Figure 14, the SCT-013 readings agreed with the reference meter within ±5% for all tested appliances. The average error was around 1-2%, with small standard deviations, indicating consistent performance. These results confirm that the SCT-013 provides sufficient accuracy for low-cost monitoring applications.

To ensure statistical validity, each measurement was repeated five times (N = 5) for each tested load. The SCT-013 showed high repeatability, with standard deviations typically below 0.025 A. The table reports both the mean error relative to the clamp ammeter and the corresponding standard deviation across repetitions.

Figure 15 demonstrates that at low currents, the relative error is high compared to medium currents (2-6 A). This phenomenon is consistent with the sensor's fixed offset and the ADC quantization effect (explained in the next section).

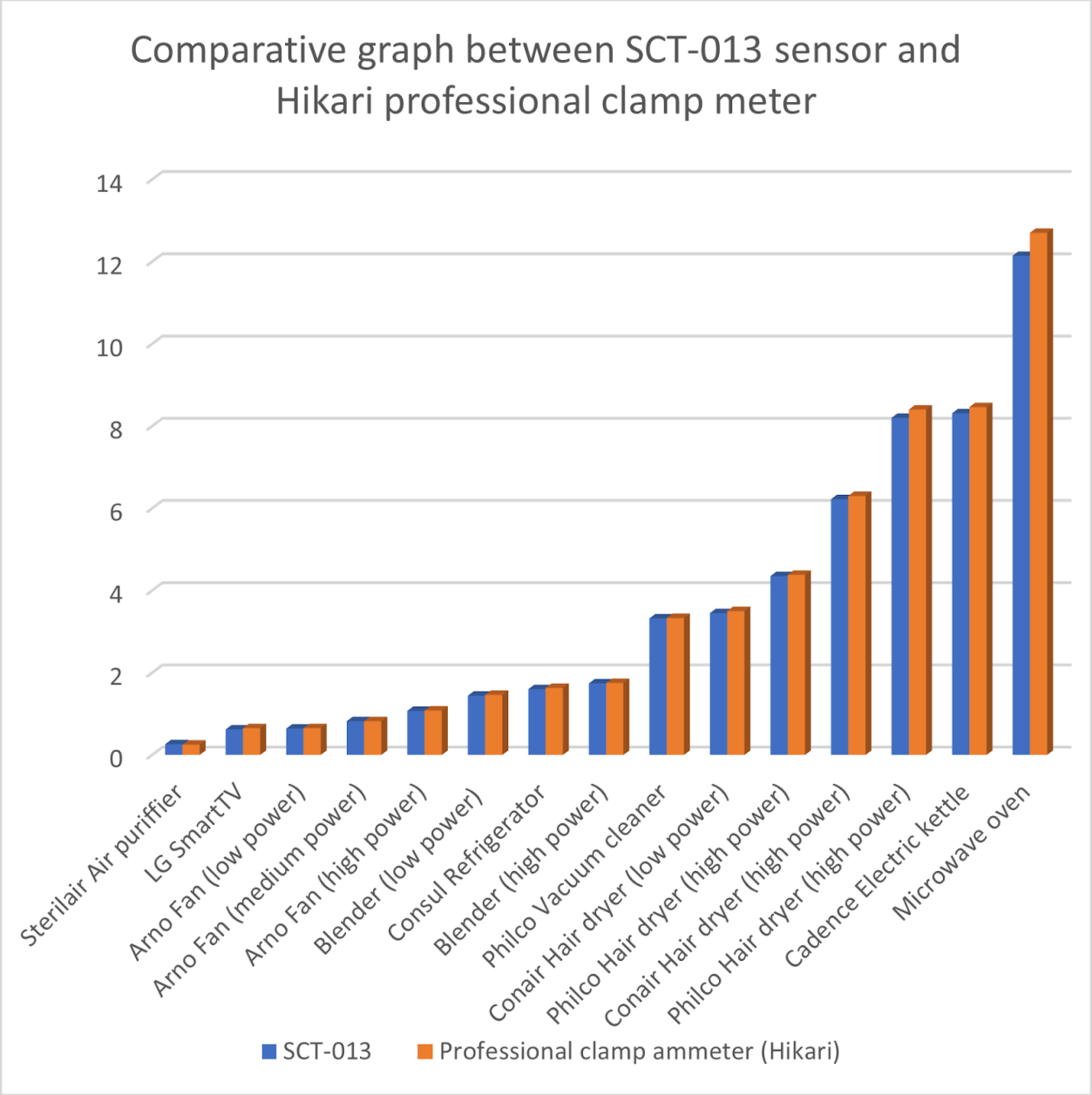

Figure 14: Comparative graph between data read by the SCT-013 sensor and the professional clamp ammeter. Source: Authors

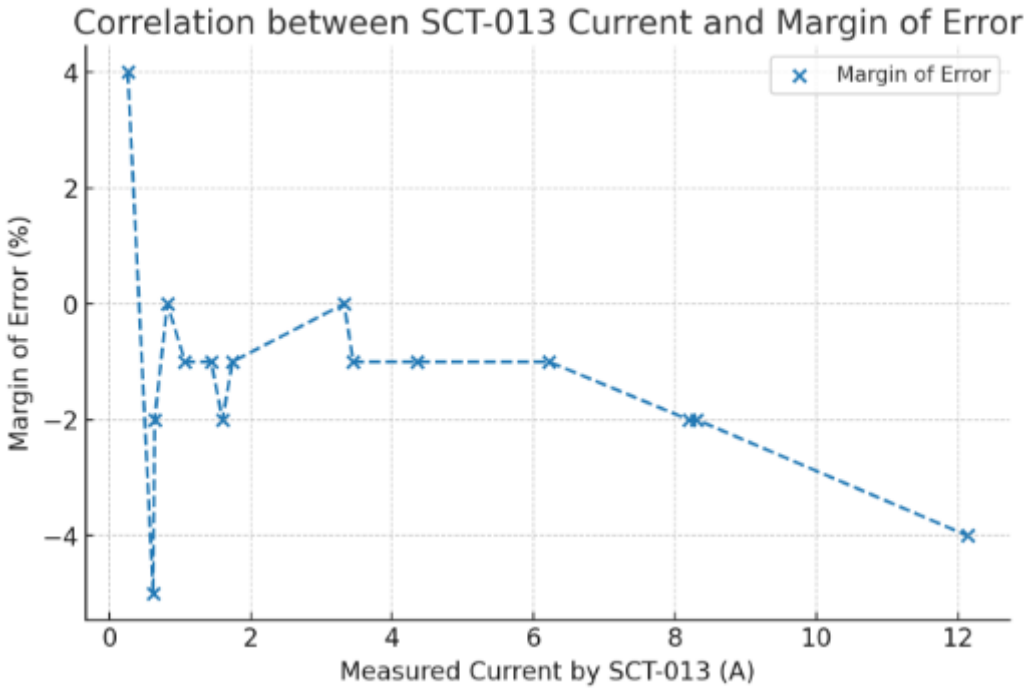

Figure 15: Correlation graph between measured current and margin of error. Source: Authors

4.1. Uncertainty Budget

The accuracy of the measurements obtained with the prototype depends on the combined performance of the sensing element, conditioning circuit, and analog-to-digital conversion stage. To assess the system's reliability, an uncertainty budget was established based on repeated laboratory tests under controlled environmental conditions. The main uncertainty contributors identified were the burden resistor characteristics, the ADC performance of the microcontroller, and the linearity of the SCT-013 current transformer.

Temperature Drift of the Burden Resistor

To characterize additional effects not included in the initial estimate, supplementary experiments were conducted to evaluate thermal drift of the burden resistor. During operation, the 33 Ω resistor dissipated approximately 0.165 W at nominal load (secondary current 70.7 mA), leading to an average temperature rise of 17 °C after 15 minutes of continuous use. Resistance increased by 0.09 Ω (0.27%), consistent with theoretical predictions for a metal-film resistor with a 50 ppm/°C temperature coefficient. Under an overload condition corresponding to double the nominal current, the power dissipation reached 0.66 W and the temperature rose by 35 °C, resulting in a resistance variation of 0.19 Ω (0.58%).

Although this drift produces only minor deviations in the measured current, it represents a relevant contribution to the

overall uncertainty, particularly under sustained or high-load operation. For the present prototype, the temperature-related contribution is estimated at ±0.3% under normal conditions and up to ±0.6% under overload. These results demonstrate that thermal effects remain small compared with the dominant linearity and tolerance components but are measurable and should be included in future calibration analyses.

ADC Non-linearity and Combined Effects

The analog-to-digital conversion represents an additional source of systematic uncertainty (Adamo et al., 2007; Zhengbing et al., 2015). The Arduino's 10-bit ADC (ATmega328P) converts analog voltages into discrete digital steps of approximately 4.88 mV per level, known as the Least Significant Bit (LSB). Its Integral Non-Linearity (INL)—the deviation between the actual and ideal conversion curve—is approximately ±2 LSB, according to the manufacturer's datasheet. The ESP32, responsible for wireless data transmission, employs a 12-bit ADC with an INL of up to ±12 LSB depending on the channel. Experimental evaluation using a calibrated 1.000 V RMS sine wave revealed deviations of ±0.4% for the Arduino and ±0.7% for the ESP32, values consistent with these specifications.

Because the Arduino is responsible for primary signal acquisition, a conservative ±0.5% ADC uncertainty was incorporated into the budget. Temperature drift and ADC non-linearity can interact, since a small rise in burden resistor voltage increases the analog input level, slightly amplifying non-linear distortion at higher ADC codes.

Combined Uncertainty and Outlook

The burden resistor (33 Ω, ±5% tolerance) and the voltage divider resistors (10 kΩ, ±1% tolerance) introduce a proportional scaling uncertainty. The Arduino ADC, with 10-bit resolution (≈4.88 mV/step over 5 V) and a typical nonlinearity of ±0.5 LSB (ATmega328P), adds quantization and transfer-curve error (Adamo et al., 2007; Zhengbing et al., 2015). The SCT-013 datasheet specifies linearity deviations up to ±3% across its nominal range. Using the root-sum-square (RSS) method, the combined type-B uncertainty is estimated at 6%, which aligns with the maximum experimental deviation observed (5%). Random errors, evaluated through repeated measurements, were comparatively small (standard deviation <0.02 A in most cases).

$$u_c = \sqrt{(5.0\%)^2 + (1.0\%)^2 + (1.0\%)^2 + (3.0\%)^2 + (0.5\%)^2 + (0.3\%)^2} = 6.02\%$$

Hence, these factors may influence accuracy in long-duration or high-temperature environments and are identified as priorities for future investigation.

4.2. Project Costs

A cost analysis of the project was conducted for potential commercial application, as seen in Table 2, and it is noted that the total cost differs from that of developing the prototype. It is important to consider that the shopping was done in Brazil, and the total cost may vary for different countries.

Table 2: Complete project cost table. Source: Authors

Installation Type	Total Cost (R$)	Total Cost (US$)	Notes
User's commercial installation	R$223.47	US$40.14	Cost of the installation used by the user
Experimental panel for testing	R$579.93	US$104.15	Constructed by the research team to simulate a house electrical panel for experiments

4.3. Limitations

As previously noted, the project initially aimed to rely solely on the ESP32 for sensor signal conversion and MQTT data transmission. However, even after recalculating the load resistor for its 3.3 V ADC, the resulting measurements showed insufficient accuracy.

$$R = V_{(analog\ input/2)}/I_{(sensor)} = 1.65\ V/0.0707\ A = 23.33\ \Omega$$

The closest commercially available resistor to the calculated value is 22 Ω.

$$CalibrationValue = number\ of\ turns\ of\ the\ sensor/value\ of\ load\ resistor$$
$$CalibrationValue = 2000/22$$
$$CalibrationValue = 90.909$$

Therefore, the sensor initialization should include the newly calculated calibration value.

```
SCT013.current(pinSCT, 90.909);
```

Even with the correct calibration values and burden resistor configuration, inaccurate measurements were being obtained when using the ESP32 alone. Measured values were off by more than 50%, and data was collected even without current passing through the SCT-013.

This discrepancy is partly attributed to the characteristics of its internal analog-to-digital converter (ADC), which is not well-suited for low-level, biased analog signals such as those produced by the SCT-013. The ESP32 ADC typically exhibits a voltage offset of approximately 0.17 V, meaning that conversions do not start at 0 V even in the absence of input (Maier et al., 2017). In addition, the ADC suffers from integral nonlinearity, channel-dependent gain variation, and sensitivity to input impedance and stability (Adamo et al., 2007; Zhengbing et al., 2015). The SCT-013 output, after passing through the burden resistor and midpoint bias network, has relatively high impedance, which can lead to unstable sampling when directly

connected to the ESP32. Small bias fluctuations can cause the ADC reference node to drift, leading to noisy or inconsistent readings, and a single calibration constant becomes unreliable across different load levels. However, with an appropriately low-impedance conditioning stage and the use of an external high-linearity ADC—such as the ADS1115—the instability can be significantly mitigated or even eliminated. In such a configuration, the ESP32 could operate as the sole microcontroller: the SCT-013 signal would be conditioned to properly drive the external ADC, which in turn would provide stable and linear digital readings to the ESP32 via I²C. In contrast, the Arduino's 10-bit ADC, though simpler, maintains a more linear and predictable transfer function over its input range, resulting in more stable and reproducible current measurements (Thakare et al., 2016). As the project is an early prototype and relies on easy and accessible approaches, acquisition and analog processing was performed on the Arduino (which exhibited more linear ADC behavior); after synchronizing the Arduino with the ESP32, the ESP32 receives the processed data and publishes it to the MQTT broker, from which the application subscribes to topics and acts as a client (Sasaki & Yokotani, 2019; Silva et al., 2021).

Another important factor to consider is that the external environment slightly affects the results collected by the sensor. For example, when the sensor is not measuring current from a conductor wire, it may still register magnetic fields emitted by nearby electronic devices. However, when there is an active current flow in the conductor, the sensor ignores this external interference and measures only the data from the intended device.

5. Conclusion

5.1. Project Conclusion

In general, the group concludes that the electric energy monitoring project successfully achieved its main objectives, demonstrating it to be an effective low-cost, modular, and accessible system capable of promoting awareness about energy consumption—the system has an accuracy of approximately 95%. This level of performance places the system within the lower bound of commercial clamp-meter solutions—typically rated between ±1% and ±3%—while remaining significantly more accessible in cost and implementation complexity. By employing a clamp-on current sensor and technologies such as Arduino, ESP32, and the MQTT protocol, it became possible to monitor energy consumption in real time from anywhere with an internet connection, thereby helping to reduce waste and encouraging more responsible electricity use (Sasaki & Yokotani, 2019; Silva et al., 2021; Tamkittikhum et al., 2015; Thakare et al., 2016).

Furthermore, from a socio-economic perspective, the project holds crucial importance as it addresses a global issue: the efficiency in electrical energy use. By monitoring energy expenditure, users can identify major points of waste and adopt more effective measures to optimize consumption. In Brazil, where electricity costs can represent a significant burden on household budgets, especially for low-income families, this technology has the potential to generate a profound positive impact. Companies and other sectors that adopt this solution can also achieve greater energy efficiency, which translates into financial savings and enhances their market competitiveness (Bento, 2024; Emanoel, 2023).

However, like any project, our system has its advantages and drawbacks. Among its main advantages, accessibility stands out, as the project can be used by diverse audiences, given that the materials employed have an affordable cost, as evinced by Table 2. Additionally, safety is a strong point, since the use of the SCT-013 sensor avoids the need to directly interfere with electrical wiring, facilitating installation and eliminating the risk of electric shocks. Another important aspect is innovation,

since the solution enables remote and real-time monitoring of energy consumption through the integration of the ESP32 with the MQTT protocol, allowing consumption tracking from anywhere in the world (Sasaki & Yokotani, 2019; Silva et al., 2021).

On the other hand, the project presents some drawbacks, such as dependence on a stable internet connection, since remote monitoring relies on a constant internet connection for data to be transmitted correctly. In locations with limited network infrastructure, the system's effectiveness may be compromised. Another shortcoming is the absence of an alert system, as the current system does not issue notifications when energy consumption exceeds certain thresholds. Moreover, the project did not implement cloud-based analysis, active response due to the high demand for energy, and multi-channel measurement, which is highly recommended for applications in complex industrial systems.

A broader reflection emerging from this work concerns the inherent trade-offs that characterize low-cost IoT sensing prototypes. The choice to pair the SCT-013 with the Arduino—rather than relying solely on the ESP32's internal ADC—illustrates a common engineering compromise between measurement accuracy, component cost, and system scalability. While the Arduino's simpler and more linear ADC offered greater stability and reproducibility for the purposes of this prototype, it also introduced additional hardware complexity and limited the potential for integration into more compact or higher-channel-count designs. Conversely, although the ESP32 provides superior processing capabilities and native wireless connectivity at a low price point, its ADC nonlinearity and impedance sensitivity constrain its use for precision analog acquisition without external conditioning. This project therefore highlights how practical IoT development often requires balancing these competing priorities rather than optimizing a single parameter in isolation.

Safety and Ethics

The system interfaces with dangerous mains voltage, so industry-standard safety measures are required. All high-voltage conductors are properly insulated and enclosed to prevent accidental contact. A suitably rated fuse is placed in series with each monitored conductor to protect against overloads. Clearance distances and insulation of materials comply with relevant electrical standards. The SCT-013 sensor provides galvanic isolation, but care is taken in circuit layout and wiring to maintain safety. On the ethical side, the device reports only aggregated energy use, not personal information, so the privacy impact is minimal. Users should still be informed that their consumption data is collected and transmitted remotely, but no sensitive personal data (e.g., identities or usage patterns per person) is exposed. It is important to note that the SCT-013 must be clamped around just one single phase conductor; otherwise, it reads opposed magnetic fields that cancel each other.

4.2. Future Implementations

For readers reproducing this work, it is recommended to expand reliability and usability in low-infrastructure contexts while preserving the system's low-cost nature. Although the current prototype already provides full offline functionality through real-time LCD visualization, future versions may incorporate non-volatile local memory (e.g., EEPROM, FRAM, or SD-card logging) to enable autonomous long-term data storage, with delayed synchronization when intermittent connectivity becomes available. To improve measurement accuracy, users reproducing the system may employ the Arduino ADC or adopt external high-linearity converters such as the ADS1115, or use an op-amp buffer; alternatively, calibration tables and oversampling techniques can be applied directly to the ESP32 to compensate for its nonlinearity and 0.17 V offset.

Additionally, since the microcontrollers support deep-sleep and periodic sampling modes, the system can operate with substantially reduced energy consumption, enabling future iterations to adopt non-intrusive powering strategies based on inductive or magnetically coupled energy-harvesting modules. Further enhancements include applying electromagnetic shielding to minimize external interference, implementing threshold-based alert systems, adding cloud-based analytics when available, and exploring AI-assisted consumption prediction and insights. These improvements would make the platform more resilient, scalable, and informative across diverse real-world environments.

6. References

Adamo, F., Attivissimo, F., Giaquinto, N., & Kale, I. (2007). Frequency domain analysis for dynamic nonlinearity measurement in A/D converters. *IEEE Transactions on Instrumentation and Measurement*, 56(3), 760–769. https://doi.org/10.1109/TIM.2007.894893

AllDataSheet. (n.d.). *SCT013 datasheet*. https://www.alldatasheet.com/datasheet-pdf/pdf/1159366/YHDC/SCT013.html

Andrade, M. (2024, September 22). Saiba quanto governo pode economizar com retorno do horário de verão. *Metrópoles*. https://www.metropoles.com/brasil/economia-br/saiba-quanto-governo-pode-economizar-com-retorno-do-horario-de-verao

Arduino. (n.d.). *analogReadResolution* [Documentation]. *Arduino Docs*. https://docs.arduino.cc/language-reference/pt/en/functions/analog-io/analogReadResolution/

Bento, W. (2024, August). Como garantir energia elétrica em lugares remotos? *Revlo*. https://revlo.com.br/como-garantir-energia-eletrica-em-lugares-remotos/

Bitencourt, R. (2024, August 20). Entenda o desafio de garantir o fornecimento de energia no Brasil no horário de pico. *Valor Econômico*. https://valor.globo.com/brasil/noticia/2024/08/20/entenda-o-desafio-de-garantir-o-fornecimento-de-energia-no-brasil-no-horario-de-pico.ghtml

Bottino, M., Nobre, P., Giarolla, E., Santos Junior, M. B., Capistrano, V. B., Malagutti, M., Tamaoki, J. N., Nobre, B. F. A., & Nobre, C. A. (2024). Amazon savannization and climate change are projected to increase dry season length and temperature extremes over Brazil. *Scientific Reports*, 14, 5131. https://doi.org/10.1038/s41598-024-55176-5

Bulhões, G., Lomba, M., & Neri, R. (2019, January). MQTT [Academic work, Departamento de Eletrônica, Escola Politécnica, Universidade Federal do Rio de Janeiro]. https://www.gta.ufrj.br/ensino/eel878/redes1-2019-1/vf/mqtt/

Emanoel. (2024, August). Importância da energia elétrica: Papel fundamental na sociedade. *Nubb*. https://nubb.com.br/importancia-da-energia-eletrica-papel-fundamental-na-sociedade-2/

Gupta, A. K., Raman, A., Kumar, N., & Ranjan, R. (2020). Design and implementation of high-speed universal asynchronous receiver and transmitter (UART). In *2020 7th International Conference on Signal Processing and Integrated Networks* (SPIN) (pp.

295–300). IEEE. https://doi.org/10.1109/SPIN48934.2020.9070856

Maier, A., Sharp, A., & Vagapov, Y. (2017). Comparative analysis and practical implementation of the ESP32 microcontroller module for the Internet of Things. In 2017 *Internet Technologies and Applications* (ITA) (pp. 143–148). IEEE. https://doi.org/10.1109/ITECHA.2017.8101926

Marengo, J. A., Alves, L. M., Alvalá, R. C. S., Cunha, A. P. M. A., Brito, S. S. B., & Moraes, O. (2018). Climatic characteristics of the 2010–2016 drought in the semiarid northeast Brazil region. *Anais da Academia Brasileira de Ciências*, 90(2 Suppl. 1), 1973–1985. https://doi.org/10.1590/0001-3765201720170206

Miron-Alexe, V. (2016). Comparative study regarding measurements of different AC current sensors. In 2016 *International Symposium on Fundamentals of Electrical Engineering* (ISFEE) (pp. 1–6). IEEE. https://doi.org/10.1109/ISFEE.2016.7803152

MQTT. (2024, August). MQTT: *The standard for IoT messaging*. https://mqtt.org/

Pfeifer, E. (2018). *Uma rede de sensores sem fio em malha para monitoramento on-line do consumo de energia nos edifícios da Universidade Federal de Santa Catarina: Um estudo de caso* (Undergraduate thesis). Universidade Federal de Santa Catarina. https://repositorio.ufsc.br/bitstream/123456789/192373/3/TCC_Eduardo_Pfeifer_ed.pdf

Rodrigues, L. (2024, September). ONS recomenda que governo volte a adotar o horário de verão. *Agência Brasil*. https://agenciabrasil.ebc.com.br/economia/noticia/2024-09/ons-recomenda-que-governo-volte-adotar-o-horario-de-verao

Rovere, R. L. D. (2016). *Protótipo de um sistema inteligente de monitoramento do consumo de energia elétrica de uma residência* (Undergraduate thesis). Universidade de São Paulo. https://bdta.abcd.usp.br/directbitstream/b3b378a1-7781-425a-800f-71d114f48f1f/Rovere_Rodrigo_Lisboa_Della_tcc.pdf

Sasaki, Y., & Yokotani, T. (2019). Performance evaluation of MQTT as a communication protocol for IoT and prototyping. *Advances in Technology Innovation*, 4(1), 21–29. https://doi.org/10.46604/aiti.2019.3000

Scianni, L. A., Queiroz, A. R., Lima, L. M. M., & Lima, J. W. M. (2013). The influence of climate change on hydro generation in Brazil. In 2013 *IEEE Grenoble Conference* (pp. 1–6). IEEE. https://doi.org/10.1109/PTC.2013.6652402

Silva, D., Carvalho, L. I., Soares, J., & Sofia, R. C. (2021). A performance analysis of Internet of Things networking protocols: Evaluating MQTT, CoAP, OPC UA. *Applied Sciences*, 11(11), 4879. https://doi.org/10.3390/app11114879

Steil, J. (2024, September 21). Afinal, vai ter horário de verão em 2024? *Valor Econômico*. https://valor.globo.com/brasil/noticia/2024/09/21/afinal-vai-ter-horario-de-verao-em-2024.ghtml

Tamkittikhun, N., Tantidham, T., & Intakot, P. (2015). AC power meter design based on Arduino: Multichannel single-phase approach. In 2015 *International Computer Science and Engineering Conference* (ICSEC) (pp. 1–5). IEEE. https://doi.org/10.1109/ICSEC.2015.7401422

Thakare, S., Shriyan, A., Thale, V., Yasarp, P., & Unni, K. (2016). Implementation of an energy monitoring and control device based on IoT. In 2016 IEEE Annual India Conference (INDICON) (pp. 1–6). IEEE. https://doi.org/10.1109/INDICON.2016.7839066

United Nations Brazil. (2024, August). *Sustainable Development Goal 7: Energia limpa e acessível*. https://brasil.un.org/pt-br/sdgs/7

Zhengbing, H., Kochan, R., Kochan, O., Jun, S., & Klym, H. (2015). Method of integral nonlinearity testing and correction of multi-range ADC by direct measurement of output voltages of multi-resistor divider. *Acta IMEKO*, 4(2), Article 14. https://doi.org/10.21014/acta_imeko.v4i2.230

Acknowledgements

To my parents, Marcelo Eduardo Xavier and Karine Furegati Dombi Xavier, and to my sister, Laura Dombi Xavier, who have supported me from an early age in my academic journey and especially throughout the research for Remote Energy Monitoring via MQTT and SCT-013: A Single-Channel Prototype for IoT Systems. To my friends, who encouraged me through every obstacle. To my teacher, Ricardo Horauti Kandi, who guided me through the academic process and provided the knowledge necessary to make this work possible. All this support was essential to my motivation throughout the entire project, and only through it was the completion of this work made possible.

Author Biography

Pedro Henrique Dombi Xavier is a 17-year-old Brazilian student at Colégio Visconde de Porto Seguro with strong interests in mechanical engineering, robotics, and accessible energy-efficiency technologies. His most recent work, “Remote Energy Monitoring via MQTT and SCT-013: A Single-Channel Prototype for IoT Systems,” proposes an open-source device capable of real-time power-consumption analysis and remote visualization. The project addresses challenges relevant to Brazil, where tariff volatility, hydro-dependence, and limited access to monitoring tools hinder efficient energy use.

Pedro’s research investigates the interaction between hardware design, analog signal acquisition, and wireless communication in IoT systems. Using clamp-on current sensing, Arduino-based ADC processing, and ESP32 MQTT transmission, he demonstrates how low-cost engineering can remain both technically rigorous and socially impactful. His work prioritizes accessibility, reproducibility, and practical innovation for communities with limited technological infrastructure. He strengthened his engineering foundation through the Engineering Summer Academy at Penn (ESAP) - Robotics, gaining hands-on experience with embedded systems, sensor integration, prototyping, motor control, and autonomous robotics. This training expanded his technical toolkit and directly informed the methodology of his energy-monitoring prototype.

Pedro is currently applying to U.S. universities to study mechanical engineering, with a particular interest in robotics, control systems, and smart-energy technologies. He aims to develop engineering solutions that promote sustainability and technological inclusion. Ultimately, he hopes to build a career at the intersection of robotics and energy systems, designing intelligent machines and sensing architectures capable of addressing structural energy challenges in countries like Brazil - making technology more efficient, equitable, and widely accessible.

Mentor Contribution Statement

Ricardo Kandi Horauti played a central role in guiding the students throughout the entire development of the research and prototype. His contributions began at the conceptual stage, where he helped the students refine the research questions, define the scope of the project, and align the work with established scientific methodologies. He provided structured guidance on how to conduct a technical literature review, evaluate prior art, and identify the conceptual gaps that the project sought to address.

A significant portion of Ricardo's contribution involved technical supervision during the construction of the electrical prototype. He worked directly with the students to assemble the wiring of the simulated distribution panel, ensuring that all components - including the current sensors, power supply, protection elements, and connection interfaces - were installed safely and correctly. Given that the project involved working with mains-level voltages, the mentor assumed responsibility for overseeing all assembly procedures, mitigating risks, and teaching safe laboratory practices. His oversight ensured that the students handled equipment properly and that all testing conditions met the necessary safety requirements.

Beyond the practical construction of the prototype, Ricardo ensured that the research adhered to scientific conventions and academic integrity standards. He reviewed each stage of the methodology to make certain that measurements, calibrations, and experimental analyses were conducted rigorously and transparently. He also assisted the students in interpreting data, validating results, and understanding the limitations of the instruments involved.

Additionally, Ricardo supported the students in structuring the manuscript, helping them communicate the theoretical background, experimental procedures, and results in a clear and academically sound manner. This included feedback on organization, clarity, and the logical progression of arguments. Throughout the process, he reinforced good research ethics, critical thinking, and responsible scientific communication.